Lateral damage in graphene carved by high energy focused gallium ion beams

Zhongquan Liao, Tao Zhang, Martin Gall, Arezoo Dianat, Rüdiger Rosenkranz, Rainer Jordan, Gianaurelio Cuniberti, and Ehrenfried Zschech

---

Articles you may be interested in

Effects of Ga ion-beam irradiation on monolayer graphene
Appl. Phys. Lett. **103**, 073501 (2013); 10.1063/1.4818458

Investigation of the effect of low energy ion beam irradiation on mono-layer graphene
AIP Advances **3**, 072120 (2013); 10.1063/1.4816715

Nanostructuring graphene on SiC by focused ion beam: Effect of the ion fluence
Appl. Phys. Lett. **99**, 083116 (2011); 10.1063/1.3628341

Ion irradiation induced structural and electrical transition in graphene
J. Chem. Phys. **133**, 234703 (2010); 10.1063/1.3518979

Damage production in semiconductor materials by a focused Ga + ion beam
J. Appl. Phys. **88**, 5658 (2000); 10.1063/1.1319168

Lateral damage in graphene carved by high energy focused gallium ion beams

Zhongquan Liao,[1,2,3,a)] Tao Zhang,[4] Martin Gall,[1] Arezoo Dianat,[3] Rüdiger Rosenkranz,[1] Rainer Jordan,[4] Gianaurelio Cuniberti,[3,5,6] and Ehrenfried Zschech[1,2]

[1]*Fraunhofer Institute for Ceramic Technologies and Systems (IKTS), Maria-Reiche-Straße 2, 01109 Dresden, Germany*
[2]*Dresden Center for Nanoanalysis (DCN), Technische Universität Dresden, Helmholtzstraße 18, 01069 Dresden, Germany*
[3]*Institute for Materials Science and Max Bergmann Center of Biomaterials, Technische Universität Dresden, Hallwachsstraße 3, 01069 Dresden, Germany*
[4]*Professur für Makromolekulare Chemie, Department Chemie, Technische Universität Dresden, Mommsenstraße 4, 01069 Dresden, Germany*
[5]*Center for Advancing Electronics Dresden (cfaed), Technische Universität Dresden, Würzburger Straße 46, 01187 Dresden, Germany*
[6]*Dresden Center for Computational Materials Science (DCCMS), Technische Universität Dresden, Hallwachsstraße 3, 01069 Dresden, Germany*

Raman mapping is performed to study the lateral damage in supported monolayer graphene carved by 30 keV focused Ga^+ beams. The evolution of the lateral damage is tracked based on the profiles of the intensity ratio between the D (1341 cm^{-1}) and G (1582 cm^{-1}) peaks (I_D/I_G) of the Raman spectra. The I_D/I_G profile clearly reveals the transition from stage 2 disorder into stage 1 disorder in graphene along the direction away from the carved area. The critical lateral damage distance spans from $<1\,\mu$m up to more than $30\,\mu$m in the experiment, depending on the parameters used for carving the graphene. The wide damage in the lateral direction is attributed to the deleterious tail of unfocused ions in the ion beam probe. The study raises the attention on potential sample damage during direct patterning of graphene nanostructures using the focused ion beam technique. Minimizing the total carving time is recommended to mitigate the lateral damage. © 2015 AIP Publishing LLC. [http://dx.doi.org/10.1063/1.4926647]

As the first isolated two-dimensional crystalline material,[1] graphene offers unprecedented opportunities in multiple research fields, e.g., photocatalysis, photoelectrocatalysis, Li-ion batteries, and so on.[2–7] Its exceptional mechanical,[8–11] electronic,[1,12–14] thermal,[15,16] and optical[17] properties promise the potential replacement of other materials in existing applications as well as completely emerging applications.

Potential applications of graphene in electronic devices and in sensors involve a sophisticated structure fabrication (patterning) in most cases.[18–21] However, considerable challenges exist in the patterning of graphene due to its single layer characteristics and the sensitivity of its intrinsic properties to geometry, residue, and damage caused by patterning.[22] So far, several methods including electron beam lithography,[23–28] atomic force microscopy,[29–32] scanning tunneling microscopy,[33,34] focused ion beam (FIB) milling,[35–43] and other techniques[44–47] were applied to pattern graphene. Among them, the FIB technique was adopted to fabricate nanostructures in various materials including biomaterials.[38] FIB milling is a highly flexible technique which allows direct and localized surface modification. Therefore, continued efforts have been devoted to developing FIB patterning for fabricating nanostructure arrays of graphene,[37,40,41,43,48–50] which is essential for the application of graphene in devices.

Raman spectroscopy is a well–established, fast, effective, and non-destructive technique to investigate the effects of defects, edges, layers, and strain on the properties of graphene.[51–58] The two most distinctive peaks in the Raman spectrum of pristine graphene are located at about 1580 (G) and 2680 (2D) cm^{-1}.[52] However, the features at about 1345 (D) and 1620 (D′) cm^{-1} can be observed too if the symmetry in graphene is disturbed due to the presence of defects and/or edges.[42,53–55,57,58] The D′ peak usually appears when the pristine graphene is heavily destructed. The ratio between the intensities of the D and G peaks (I_D/I_G) provides abundant information about the density of defects and the evolution of disorder.[42,53]

In the current study, focused Ga^+ ions are used in a scanning electron microscopy (SEM)/FIB tool to modify graphene. Various beam currents and doses are chosen to bombard the graphene. Material modifications, especially the wide lateral damage in graphene in the surrounding of the irradiated target area, are characterized using Raman spectroscopy. Such wide lateral damage observed in the study has not been well realized before and should address a concern of the lateral implantation of ions on the patterned graphene micro- and nano-structures when directly using the FIB technique. The study also provides a different insight to understand the origin of the lateral damage, which was misunderstood or not well explained.

Monolayer graphene samples were produced in a chemical vapor deposition (CVD) furnace using copper as the

a)Author to whom correspondence should be addressed. Electronic mail: zhongquan.liao@ikts-md.fraunhofer.de.

107, 013108-1

catalyst and the substrate, and then were transferred to a Si/SiO$_2$ wafer using polymethyl methacrylate (PMMA) method.[59,60] Ion bombardment was performed in a SEM/FIB tool (Carl Zeiss NVision 40). The ion bombardment was performed "blindly" to avoid any unnecessary damage on graphene from the rough ion imaging. A confocal Raman microscope (NT-MDT) was used to evaluate the effect of the ions on the graphene. The Raman spectrum was excited by a 532 nm (2.33 eV) laser, and the spot size of the laser beam was about 0.5 μm. Molecular dynamics (MD) simulations were used to simulate the ion beam irradiation induced damage on the graphene supported by the SiO$_2$ substrate. Details of the MD simulation are provided in the supplementary material.[61]

Fig. 1(a) shows the optical image of a monolayer graphene with a 4.5 μm × 5.8 μm rectangle (indicated by a red arrow) carved by a Ga$^+$ ion beam. The acceleration voltage for the Ga$^+$ ions and the applied current were 30 kV and 1 pA, respectively. For a bombardment time of 30 s, the totally applied ion dose was 7.18×10^{14} ions/cm^2. The notable region outside the carved area, as observed in all three Raman mappings (Figs. 1(b)–1(d)), indicates a wide range of disordered graphene caused by the Ga$^+$ ion beam. This affected region in the Raman mapping of $I_{D'}$ is much smaller than that in the Raman mappings of I_D and I_D/I_G. Since the D$'$ peak usually appears when the pristine graphene is heavily destructed, it indicates that the graphene very close (about

1.5 μm) to the carved rectangle was heavily destructed and may contain a very high degree of defects, disorder, or even amorphous fraction. However, a slight damage of graphene is extended to a few more μm away from the rectangle (Figs. 1(b) and 1(d)).

In order to track the evolution of the lateral damage in the carved graphene, eight representative Raman spectra (Fig. 1(e)) were extracted from the original Raman mapping data at several positions, which are labeled by numbers from 1 to 8 in Fig. 1(d). The corresponding Raman features from the spectra are summarized in Table I. Spectrum 1 without any characteristic peaks of the graphene confirms that the graphene was completely etched away by the Ga$^+$ ions in the target rectangle. In the region next to the carved rectangle, spectrum 2 shows no characteristic 2D peak, but a clear D peak and a broad G peak with a ratio $I_D/I_G \sim 2.66$. It indicates that the graphene was seriously amorphized in this region.[53] Spectrum 3 shows a typical Raman spectrum in the yellow/red colored region (see Fig. 1(d)). All four peaks, i.e., D, G, D$'$, and 2D are present in the spectrum, and the ratio of I_D/I_G is $\sim$3.99, which is a good indication of the highly disordered graphene. From the spectra of the position 4, 5, 6, and 7, it is found that both the intensities of the D peak and the D$'$ peak monotonically decrease as a function of distance from the carved rectangle. The ratios of I_D/I_G for spectra 4, 5, 6, and 7 are 2.61, 1.75, 0.97, and 0.56, respectively. The D$'$ peak is negligible in spectrum 7; however, the corresponding D peak is still significant even the position for spectrum 7 is 6.2 μm away from the carved boundary. For position 8, which is more than 15 μm away from the carved boundary, a very slight D peak appears. This feature could easily be observed in the transferred CVD graphene grown on Cu. The FWHM of the G peak is about 32 cm^{-1}, the ratio of intensities between the 2D and G peak is 2.3 ± 0.1. All features are similar to the ones in the Raman spectrum of the pristine monolayer graphene, which implies no detectable damage of graphene caused by the ions.

Fig. 1(f) shows the average damage (I_D/I_G) profiles as a function of distance away from the carved area, both profiles show a very good consistency. There are two stages of disorder in graphene (described by a local activation model), which were experimentally observed and reported in Refs. 42,53,57, and 62, where the I_D/I_G should increase with the defect density in stage 1 and start decreasing in stage 2 due
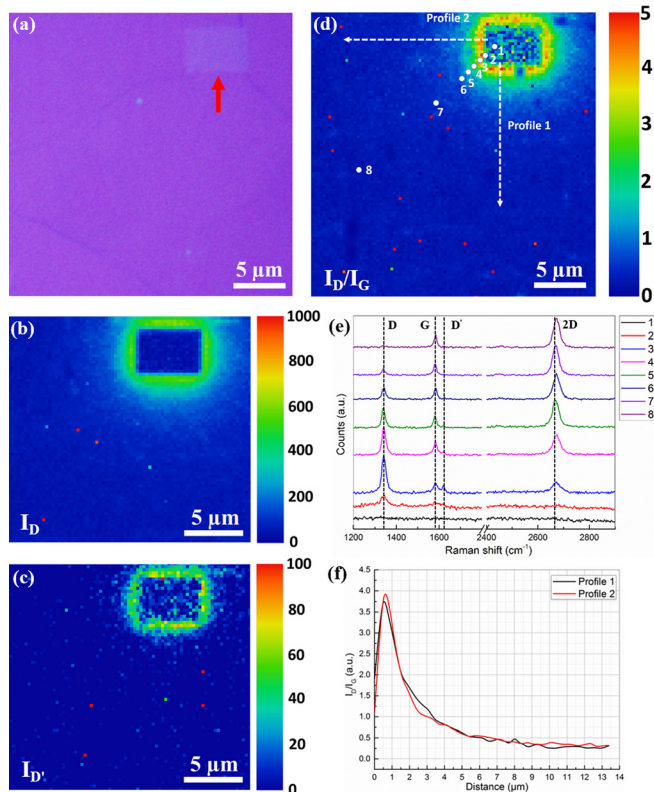

FIG. 1. (a) Optical image of a monolayer graphene with a 4.5 μm × 5.8 μm rectangle carved by a Ga$^+$ ion beam (30 kV, 1 pA/30 s, and 7.18×10^{14} ions/cm^2 dose). (b)–(d) The corresponding Raman mappings of I_D, $I_{D'}$, and I_D/I_G from the carved graphene. (e) The Raman spectra of the carved graphene at different positions marked in Fig. 1(d). (f) The mean damage (I_D/I_G) plots as a function of distance from the carved area (indicated by two white dashed arrows in Fig. 1(d)).

TABLE I. Raman features summarized from the spectra in Fig. 1(e).

Position (distance from the carved region)/ Raman feature	D (1341 cm^{-1})	G (1582 cm^{-1})	D$'$ (1621 cm^{-1})	2D (2671 cm^{-1})	I_D/I_G
1 (within the carved region)	No	No	No	No	NA
2 (0.13 μm)	Yes	Yes	No	No/negligible	2.66
3 (0.52 μm)	Yes	Yes	Yes	Yes	3.99
4 (1.29 μm)	Yes	Yes	Yes	Yes	2.61
5 (2.06 μm)	Yes	Yes	Yes	Yes	1.75
6 (3.14 μm)	Yes	Yes	Yes	Yes	0.97
7 (6.20 μm)	Yes	Yes	No/negligible	Yes	0.56
8 (>15 μm)	Yes	Yes	No/negligible	Yes	0.15

to the loss of hexagonal rings. The I_D/I_G data shown in Fig. 1(f) demonstrate a similar non-monotonic tendency: in the regions far from the carved rectangle, it follows the characteristics of stage 1 disorder, i.e., the I_D/I_G increases with the decrease of the distance due to the increase of the defect density; in the regions close to the carved rectangle, it shows the characteristics of stage 2 disorder, i.e., the I_D/I_G decreases with the decrease of the distance due to the loss of hexagonal rings. The profiles clearly reveal that the lateral damage (stage 1 disorder) in graphene extends to about 8.5 μm from the carved structure until reaching the pristine region.

Fig. 2 shows the Raman mappings of I_D/I_G of graphene carved by Ga^+ ions with several different parameters and the corresponding mean damage (I_D/I_G ratio) profiles. All Raman mappings of the I_D/I_G ratio show a damaged region with a radial dependency outside the carved rectangle. A summary of FIB current, irradiation time, ion dose, and critical lateral damage distance for each bombarded rectangle is shown in Table II. For the same ion beam current (1 pA), the critical lateral damage distance significantly increases from 0.63 ± 0.25 μm to 8.40 ± 0.30 μm while increasing the irradiation time from 5 s to 300 s (ion dose from 1.20×10^{14} ions/cm^2 to 7.18×10^{15} ions/cm^2). Rectangle 4 was carved by an ion beam with 10 times of the dose used for rectangle 2, while with 1/10 of the irradiation time used for rectangle

3. Since the Ga^+ ion beam size is proportional to the beam current,[38] for the 10 pA beam current used for rectangle 4, it is supposed to generate a larger ion spot than for the 1 pA beam current used for rectangles 2 and 3. Surprisingly, rectangle 4 shows much less lateral damage than rectangle 3 (8.40 ± 0.30 μm for rectangle 3 and 3.45 ± 0.30 μm for rectangle 4). Since it only shows a slight increase of the lateral damage compared to rectangle 2 (2.69 ± 0.26 μm for rectangle 2 and 3.45 ± 0.30 μm for rectangle 4), the bombardment time obviously plays a more important role than the ion current for the lateral damage in graphene, for relatively low ion beam current. However, 80 pA beam current is not suitable for carving micro- and nano-structures in graphene because the observed lateral damage extended to more than 30 μm away from the carved structure, even for very short irradiation time (10 s).

Both the Monte Carlo simulation of the trajectories and collision cascades of 30 keV Ga^+ ions impinging into Si and the direct calculation of 30 keV Ga^+ ion beam propagation into graphene on a Si/SiO$_2$ substrate showed that the interaction distance in the lateral direction is in the range of 100 nm only.[37,38] A MD simulation was also conducted to simulate the irradiation damage in graphene supported on the SiO$_2$ substrate, as shown in Fig. 3. The damage of graphene is very localized by either a focused Ga^+ ion beam or
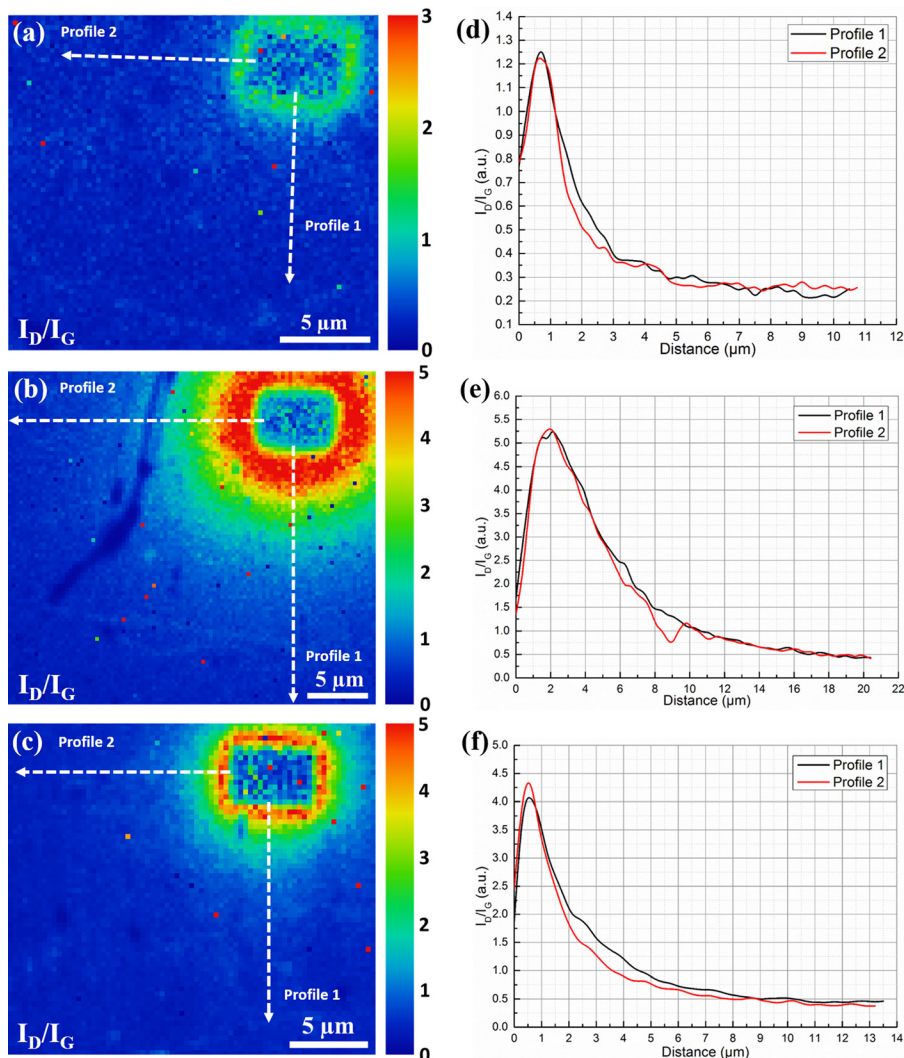

FIG. 2. (a)–(c) Raman mappings of I_D/I_G from the carved graphene by different Ga^+ ion beams and (d)–(f) the corresponding mean damage (I_D/I_G) plots as a function of distance from the carved area (indicated by white dashed arrows). (The parameters for the Ga^+ ion beams used in different samples: (a) and (d) 30 kV, 1 pA/5 s, and 1.20×10^{14} ions/cm^2 dose; (b) and (e) 30 kV, 1 pA/300 s, and 7.18×10^{15} ions/cm^2 dose; (c) and (f) 30 kV, 10 pA/30 s, and 7.18×10^{15} ions/cm^2 dose.)

TABLE II. A summary of FIB current, irradiation time, ion dose, and critical lateral damage distance for each bombarded rectangle.

Rectangle	1	2	3	4	5
FIB current (pA)	1	1	1	10	80
Irradiation time (s)	5	30	300	30	10
Dose (ions/cm^2)	1.20×10^{14}	7.18×10^{14}	7.18×10^{15}	7.18×10^{15}	1.92×10^{16}
Critical lateral damage distance[a] (μm)	0.63 ± 0.25	2.69 ± 0.26	8.40 ± 0.30	3.45 ± 0.30	>30[b]

[a]Critical lateral damage distance (obtained from the Raman mapping of I_D/I_G): the distance of the damage value (I_D/I_G) from maximum to 1 in an I_D/I_G profile from a carved rectangle.

[b]This data was obtained from a rough estimate by directly observing the bombarded graphene sample in the Raman microscope, not from the Raman mapping.

by a beam with slightly diffused ions. That means, theoretically, the focused Ga$^+$ ion beam should not generate such a wide lateral damage in graphene. However, the ion probe profile in commercial FIB tools follows approximately a Gaussian shape.[63] Therefore, the deleterious tail consisting of unfocused ions in the probe has to be considered. Although it is not feasible to simulate a Gaussian shape ion beam in the molecular dynamics simulation, as shown in Figs. 3(c) and 3(d), the beam with slightly diffused Ga$^+$ ions creates a slightly higher degree of damage in the graphene compared to the tightly focused beam. It supports the experimental result that the damage is expanded to a large area if the ion beam has an unfocused deleterious tail. The supplementary material[61] also provides an indirect support. Although the graphene outside the irradiated area could be preserved due to the low dose of ions in the deleterious tail of the ion beam probe, the preserved material may not be called as graphene because of the heavily damaged

FIG. 3. Molecular dynamics simulations of the damage in the graphene by 30 keV Ga$^+$ ion beams. (a) and (b) Illustration of the simulation setup for the ion bombardment of graphene supported by the SiO$_2$ substrate; (a) a sharp beam, (b) a beam with slightly diffused ions. (c) and (d) The corresponding damaged graphene after ion bombardment by the sharp beam (c) and the beam with slightly diffused ions (d). The dark red, dark blue, red, and yellow balls represent the Ga$^+$ ions and the C, O, and Si atoms, respectively.

characteristic observed by Raman spectroscopy and transmission electron microscopy.[61]

For 1 pA beam current, the FIB-induced lateral damage extends to up to ∼18.5 μm shown in Figs. 2(b) and 2(e), which proves that the tail of unfocused ions in the probe extends to an unexpected far distance in the lateral direction. The damaged region in graphene is dramatically reduced due to the reduction of time for the ion bombardment in Figs. 2(a) and 2(d), and for distances of about ∼5 μm and more from the carved structure only a slight defective characteristics is observed. It is inferred that the ion beam current density is extremely low at the end of the tail even though the tail of unfocused ions in the probe covers a large area, a detectable lateral damage in graphene by Raman microscopy only appears after a relatively long time of bombardment. Thus, minimizing the total milling time during the direct patterning is highly recommended to reduce the deleterious lateral damage in graphene. Another interesting phenomenon is that the percentage of the dose for unfocused ions (unwanted tail) in the primary ion beam varies with the ion current, as shown in Figs. 2(b) and 2(c). The percentage of the dose for unfocused ions at 10 pA beam current is much lower than that at 1 pA beam current, since the graphene carved by the 10 pA ion beam shows much less lateral damage when using the same dose from the primary ion beam (rectangles 3 and 4 in Table II). The lateral spreading of the ion beam damage found here is consistent with the results reported in the Refs. 64 and 65. It is not surprising that a wider affected region of graphene is observed, due to its characteristics of single atomic layer and the high sensitivity to detect the defects in graphene by Raman spectroscopy.

In summary, the lateral damage in graphene carved by a 30 keV Ga$^+$ beam was studied using Raman spectroscopy. Severe and reproducible lateral damage in graphene outside the carved area was observed. The mean damage (I_D/I_G) profiles reveal the clear transition from stage 2 disorder into stage 1 disorder in graphene along the direction away from the carved area. The critical lateral damage distance is 8.40 ± 0.30 μm when using a 1 pA/300 s (7.18×10^{15} ions/cm^2) beam, and extends to more than 30 μm using extreme parameters. This value is reduced to 0.63 ± 0.25 μm with a short carving time (5 s) at 1 pA beam current. This laterally extended damage is caused by the deleterious tail of the Ga$^+$ ion beam, consisting of unfocused ions. The lateral damage has to be considered in direct patterning of graphene nanostructures using the FIB technique. Minimizing the total carving time will be the recommended approach to minimize the lateral damage.
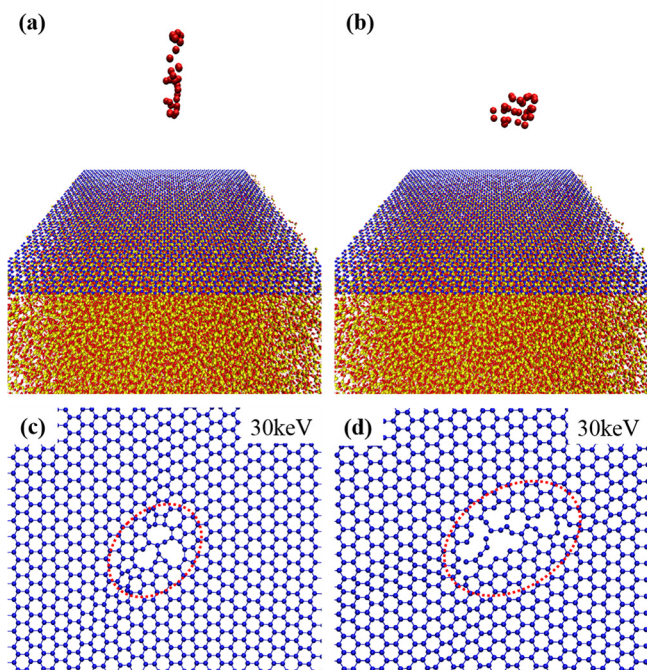
[1]A. K. Geim and K. S. Novoselov, Nat. Mater. **6**, 183 (2007).

[2]W. J. Ong, L. L. Tan, S. P. Chai, and S. T. Yong, Chem. Commun. **51**, 858 (2015).

[3]H. Xu, P. Wu, C. Liao, C. Lv, and Z. Gu, Chem. Commun. **50**, 8591 (2014).

[4]Y. T. Xu, Y. Guo, C. Li, X. Y. Zhou, M. C. Tucker, X. Z. Fu, R. Su, and C. P. Wong, Nano Energy **11**, 38 (2015).

[5]D. Yoo, J. Kim, and J. H. Kim, Nano Res. **7**, 717 (2014).

[6]W. J. Ong, L. L. Tan, S. P. Chai, S. T. Yong, and A. R. Mohamed, Nano Res. **7**, 1528 (2014).

[7]W. J. Ong, S. Y. Voon, L. L. Tan, B. T. Goh, S. T. Yong, and S. P. Chai, Ind. Eng. Chem. Res. **53**, 17333 (2014).

[8]P. Y. Huang, C. S. Ruiz-Vargas, A. M. Zande, W. S. Whitney, M. P. Levendorf, J. W. Kevek, S. Garg, J. S. Alden, C. J. Hustedt, Y. Zhu, J. Park, P. L. McEuen, and D. A. Muller, Nature **469**, 389 (2011).

[9]C. Lee, X. Wei, J. W. Kysar, and J. Hone, Science **321**, 385 (2008).

[10]G. H. Lee, R. C. Cooper, S. J. An, S. Lee, A. Zande, N. Petrone, A. G. Hammerberg, C. Lee, B. Crawford, W. Oliver, J. W. Kysar, and J. Hone, Science **340**, 1073 (2013).

[11]H. I. Rasool, C. Ophus, W. S. Klug, A. Zettl, and J. K. Gimzewski, Nat. Commun. **4**, 2811 (2013).

[12]S. V. Morozov, K. S. Novoselov, M. I. Katsnelson, F. Schedin, D. C. Elias, J. A. Jaszczak, and A. K. Geim, Phys. Rev. Lett. **100**, 016602 (2008).

[13]H. B. Heersche, P. Jarillo-Herrero, J. B. Oostinga, L. M. K. Vandersypen, and A. Morpurgo, Nature **446**, 56 (2007).

[14]K. S. Novoselov, A. K. Geim, S. V. Morozov, D. Jiang, Y. Zhang, S. V. Dubonos, I. V. Grigorieva, and A. A. Firsov, Science **306**, 666 (2004).

[15]A. A. Balandin, Nat. Mater. **10**, 569 (2011).

[16]E. Pop, V. Varshney, and A. K. Roy, MRS Bull. **37**, 1273 (2012).

[17]R. R. Nair, P. Blake, A. N. Grigorenko, K. S. Novoselov, T. J. Booth, T. Stauber, N. M. R. Peres, and A. K. Geim, Science **320**, 1308 (2008).

[18]K. S. Novoselov, D. Jiang, F. Schedin, T. J. Booth, V. V. Khotkevich, S. V. Morozov, and A. K. Geim, Proc. Natl. Acad. Sci. U. S. A. **102**, 10451 (2005).

[19]K. S. Novoselov, V. I. Falko, L. Colombo, P. R. Gellert, M. G. Schwab, and K. Kim, Nature **490**, 192 (2012).

[20]Q. Yan, B. Huang, J. Yu, F. Zheng, J. Zang, J. Wu, B. Gu, F. Liu, and W. Duan, Nano Lett. **7**, 1469 (2007).

[21]X. Liang and S. Wi, ACS Nano **6**, 9700 (2012).

[22]K. S. Novoselov, Z. Jiang, Y. Zhang, S. V. Morozov, H. L. Stormer, U. Zeitler, G. S. Boebinger, P. Kim, and A. K. Geim, Science **315**, 1379 (2007).

[23]M. Y. Han, B. Ozyilmaz, Y. Zhang, and P. Kim, Phys. Rev. Lett. **98**, 206805 (2007).

[24]S. Heydrich, M. Hirmer, C. Preis, T. Korn, J. Eroms, D. Weiss, and C. Schüller, Appl. Phys. Lett. **97**, 043113 (2010).

[25]Y. Lu, C. A. Merchant, M. Drndic, and A. T. C. Johnson, Nano Lett. **11**, 5184 (2011).

[26]M. D. Fischbein and M. Drndic, Appl. Phys. Lett. **93**, 113107 (2008).

[27]F. Börrnert, L. Fu, S. Gorantla, M. Knupfer, B. Büchner, and M. H. Rümmeli, ACS Nano **6**, 10327 (2012).

[28]Z. J. Qi, J. A. Rodriguez-Manzo, A. R. Botello-Mendez, S. J. Hong, E. A. Stach, Y. W. Park, J. C. Charlier, M. Drndic, and A. T. C. Johnson, Nano Lett. **14**, 4238 (2014).

[29]L. Weng, L. Zhang, Y. P. Chen, and L. P. Rokhinson, Appl. Phys. Lett. **93**, 093107 (2008).

[30]S. Masubuchi, M. Ono, K. Yoshida, K. Hirakawa, and T. Machida, Appl. Phys. Lett. **94**, 082107 (2009).

[31]R. K. Puddy, P. H. Scard, D. Tyndall, M. R. Connolly, C. G. Smith, G. A. C. Jones, A. Lombardo, A. C. Ferrari, and M. R. Buitelaar, Appl. Phys. Lett. **98**, 133120 (2011).

[32]Y. Zhang, Y. Gao, L. Liu, N. Xi, Y. Wang, L. Ma, Z. Dong, and U. C. Wejinya, Appl. Phys. Lett. **101**, 213101 (2012).

[33]L. Tapaszto, G. Dobrik, P. Lambin, and L. P. Biro, Nat. Nanotechnol. **3**, 397 (2008).

[34]P. Nemes-Incze, L. Tapaszto, G. Zs. Magda, Z. Osvath, G. Dobrik, X. Jin, C. Hwang, and L. P. Biro, Appl. Surf. Sci. **291**, 48 (2014).

[35]D. Lucot, J. Gierak, A. Ouerghi, E. Bourhis, G. Faini, and D. Mailly, Microelectron. Eng. **86**, 882 (2009).

[36]M. C. Lemme, D. C. Bell, J. R. Williams, L. A. Stern, B. W. H. Baugher, P. Jarillo-Herrero, and C. M. Marcus, ACS Nano **3**, 2674 (2009).

[37]D. C. Bell, M. C. Lemme, L. A. Stern, J. R. Williams, and C. M. Marcus, Nanotechnology **20**, 455301 (2009).

[38]N. Bassim, K. Scott, and L. A. Giannuzzi, MRS Bull. **39**, 317 (2014).

[39]A. Morin, D. Lucot, A. Querghi, G. Patriarche, E. Bourhis, A. Madouri, C. Ulysse, J. Pelta, L. Auvray, R. Jede, L. Bruchhaus, and J. Gierak, Microelectron. Eng. **97**, 311 (2012).

[40]Y. Zhang, C. Hui, R. Sun, K. Li, K. He, X. Ma, and F. Liu, Nanotechnology **25**, 135301 (2014).

[41]B. S. Archanjo, A. P. M. Barboza, B. R. A. Neves, L. M. Malard, E. H. M. Ferreira, J. C. Brant, E. S. Alves, F. Plentz, V. Carozo, B. Fragneaud, I. O. Maciel, C. M. Almeida, A. Jorio, and C. A. Achete, Nanotechnology **23**, 255305 (2012).

[42]S. Hang, Z. Moktadir, and H. Mizuta, Carbon **72**, 233 (2014).

[43]K. Celebi, J. Buchheim, R. M. Wyss, A. Droudian, P. Gasser, I. Shorubalko, J. Kye, C. Lee, and H. G. Park, Science **344**, 289 (2014).

[44]L. C. Campos, V. R. Manfrinato, J. D. Sanchez-Yamagishi, J. Kong, and P. Jarillo-Herrero, Nano Lett. **9**, 2600 (2009).

[45]C. X. Cong, T. Yu, Z. H. Ni, L. Liu, Z. X. Chen, and W. Huang, J. Phys. Chem. C **113**, 6529 (2009).

[46]M. J. Allen, V. C. Tung, L. Gomez, Z. Xu, L. Chen, K. S. Nelson, C. Zhou, R. B. Kaner, and Y. Yang, Adv. Mater. **21**, 2098 (2009).

[47]Y. Zhou, Q. Bao, B. Varghese, L. Tang, T. Khim, C. Sow, and K. Loh, Adv. Mater. **22**, 67 (2010).

[48]B. Prevel, J. M. Benoit, L. Bardotti, P. Melinon, A. Ouerghi, D. Lucot, E. Bouurhis, and J. Gierak, Appl. Phys. Lett. **99**, 083116 (2011).

[49]B. S. Archanjo, B. Fragneaud, L. G. Cancado, D. Winston, F. Miao, C. A. Achete, and G. Medeiros-Ribeiro, Appl. Phys. Lett. **104**, 193114 (2014).

[50]N. Kalhor, S. A. Boden, and H. Mizuta, Microelectron. Eng. **114**, 70 (2014).

[51]A. C. Ferrari, J. C. Meyer, V. Scardaci, C. Casiraghi, M. Lazzeri, F. Mauri, S. Piscanec, D. Jiang, K. S. Novoselov, S. Roth, and A. K. Geim, Phys. Rev. Lett. **97**, 187401 (2006).

[52]A. C. Ferrari and D. M. Basko, Nat. Nanotechnol. **8**, 235 (2013).

[53]M. M. Lucchese, F. Stauale, E. H. M. Ferreira, C. Vilani, M. V. O. Moutinho, R. B. Capaz, C. A. Achete, and A. Jorio, Carbon **48**, 1592 (2010).

[54]S. Ryu, J. Maultzsch, M. Y. Han, P. Kim, and L. E. Brus, ACS Nano **5**, 4123 (2011).

[55]M. Huang, Y. Hugen, T. F. Heinz, and J. Hone, Nano Lett. **10**, 4074 (2010).

[56]O. Frank, G. Tsoukleri, J. Parthenios, K. Papagelis, I. Riaz, R. Jalil, K. S. Novoselov, and C. Galiotis, ACS Nano **4**, 3131 (2010).

[57]G. Liu, D. Teweldebrhan, and A. A. Balandin, IEEE Trans. Nanotechnol. **10**, 865 (2011).

[58]M. Xu, D. Fujita, and N. Hanagata, Nanotechnology **21**, 265705 (2010).

[59]S. Bae, H. Kim, Y. Lee, X. Xu, J. S. Park, Y. Zheng, J. Balakrishnan, T. Lei, H. Ri Kim, Y. L. Song, Y. J. Kim, K. S. Kim, B. Ozyilmaz, J. H. Ahn, B. H. Hong, and S. Iijima, Nat. Nanotechnol. **5**, 574 (2010).

[60]X. Li, W. Cai, J. An, S. Kim, J. Nah, D. Yang, R. Piner, A. Velamakanni, I. Jung, E. Tutuc, S. K. Banerjee, L. Colombo, and R. S. Ruoff, Science **324**, 1312 (2009).

[61]See supplementary material at http://dx.doi.org/10.1063/1.4926647 for the details of the MD simulation used to simulate the ion beam irradiation induced damage on the graphene supported by the SiO_2 substrate, the TEM study on a graphene ribbon carved by a high energy focused Ga^+ ion beam, and the AFM results for the graphene supported on the Si/SiO$_2$ wafer with a rectangle carved by a high energy focused Ga^+ ion beam.

[62]L. G. Cancado, A. Jorio, E. H. Martins Ferreira, F. Stavale, C. A. Achete, R. B. Capaz, M. V. O. Moutinho, A. Lombardo, T. S. Kulmala, and A. C. Ferrari, Nano Lett. **11**, 3190 (2011).

[63]G. B. Assayag, C. Vieu, J. Gierak, P. Sudraud, and A. Corbin, J. Vac. Sci. Technol., B **11**, 2420 (1993).

[64]J. Gierak, G. B. Assayag, M. Schneider, C. Vieu, and J. Y. Marzin, Microelectron. Eng. **30**, 253 (1996).

[65]T. Yamamoto, J. Yanagisawa, K. Gamo, S. Takaoka, and K. Murase, Jpn. J. Appl. Phys., Part 1 **32**, 6268 (1993).